Quim. Nova, Vol. 32, No. 7, 1812-1817, 2009

Artigo

SYNTHESIS, CHARACTERIZATION, DFT AND TD-DFT STUDY OF THE [Fe(mnt)(L)(*t*-BuNC)$_2$] OCTAHEDRAL COMPLEX (L = phen, bipy)

Milton K. Morigaki*, Elias M. da Silva, Carlos V. P. de Melo, Jamile R. Pavan e Renzo C. Silva
Departamento de Química, Universidade Federal do Espírito Santo, Av. Fernando Ferrari, s/n, 29060-900 Vitória – ES, Brasil
Armando Biondo e Jair C. C. Freitas
Departamento de Física, Universidade Federal do Espírito Santo, 29060-900 Vitória – ES, Brasil
Gilson H. M. Dias
Instituto de Química, Universidade Estadual de Campinas, CP 6154, 13084-971 Campinas – SP, Brasil

Recebido em 12/9/08; aceito em 8/4/09; publicado na web em 26/8/09

$FeBr_2$ has reacted with an equivalent of mnt^{2-} (mnt = *cis*-1,2-dicyanoethylene-1,2-dithiolate) and the α-diimine L (L = 1,10'-phenantroline, 2,2'-bipyridine) in THF solution, and followed by adding of *t*-butyl-isocyanide to give [Fe(mnt)(L)(*t*-BuNC)$_2$] neutral compound. The products were characterized by infrared, UV-visible and Mössbauer spectroscopy, besides thermogravimetric and conductivity data. The geometry in the equilibrium was calculated by the density functional theory and the electronic spectrum by the time-dependent. The experimental and theoretical results in good agreement have defined an octahedral geometry with two isocyanide neighbours. The $\pi \rightarrow \pi^*$ intraligand electronic transition was not observed for *cis*-isomers in the near-IR spectral region.

Keywords: iron(II); isocyanide; DFT.

INTRODUCTION

Transition metal complexes with an oxidizing and a reducing ligand have the fascinating physical properties and electronic structures are frequently characterized by low-energy transitions between HOMO/LUMO. In suitable case, the involvement of the dithiolate (mnt) donor-ligand and of the α-diimine acceptor-ligand in the coordination sphere facilitates ready movement of electrons between HOMO and LUMO. For this reason is that some [M(α-diimine)(dithiolate)] square-planar transition metal compounds containing a mutually *trans* arrangement diimine and dithiolate ligands have multiple accessible redox states[1] with high degree of electron delocalization. Therefore, they can exhibit the common low-energy charge transfer term, which is a condition to be photocatalist chromophores for solar energy conversion and storage.[2] Iron-sulfur compounds with ancillary isocyanide ligands cause structural systematic changes with a concomitant strong effect on the chemical properties,[3,4] besides have an active center in biochemical processes,[5,6] could also display features of the proteins and [M(α-diimine)(dithiolate)] counterparts.

The work presented herein toward a comprehensive description of novel octahedral products with α-diimine chelating ligands is a continuation of our previous studies on the nature of the iron compounds containing mnt-isocyanide ligands.[7]

EXPERIMENTAL

Experiments were performed under argon atmosphere, using standard Schlenk techniques to avoid the oxidation process. The solvents were dried and distilled under O_2-free argon prior to use. The compounds *t*-BuNC,[8] $FeBr_2$[9] and Na_2mnt[10] were prepared as previously described. The phen and the bipy were purchased from Aldrich and used as received.

IR spectra were obtained on a Midac Prospect FT-IR instruments, using Nujol mulls. Melting points were recorded on a Büchi 510 apparatus and are uncorrected. Elemental analyses (C, H, and N) were performed on a Perkin Elmer 2400 microanalytical instrument. Optical absorption spectra were obtained on Varian Cary 1, using THF solution. Conductivities were measured at 25 ºC, using a HANNA Instruments HI 8033 conductivity bridge and standard cell. For the Mössbauer measurements, the usual transmission geometry was employed, with an Ortec multichannel system PC board, using 512 channels, as the data counting. The gamma rays source was a nominal 10 mCi ^{57}Co in a Pd or Rh matrix and the isomer shift values are quoted relative to α-Fe. Thermogravimetric (TG) curves were recorded with a Shimadzu TGA-50H thermal analyser system. The samples with initial mass around 12 mg were heated in alumina crucible under oxygen flow (20 cm^3 min^{-1}) at a heating rate of 10.0 ºC min^{-1}.

Preparation of [Fe(mnt)(phen)(*t*-BuNC)$_2$] (1)

Small portions of Na_2mnt (0.400 g, 2.15 mmol) and phen (0.387 g, 2.15 mmol) were added to a stirred solution of $FeBr_2$ (0.464 g, 2.15 mmol) in THF (45 cm^3). To the stirring mixture was added *t*-BuNC (0.58 cm^3, 5.2 mmol). After 2h, the resulting solution was filtered through a Florisil column and concentrated to *ca*. 4 cm^3. Dropwise addition of diethyl ether (10 cm^3) afforded a brown solid, which was washed with diethyl ether (3 x 3 cm^3 portions), and vacuum-dried. Yield 40%. (Found: C, 56.5; H, 5.3; N, 15.5. $C_{24}H_{26}S_2FeN_6$ requires C, 57.6; H, 4.8; N, 15.5%). IR ν(CN) (Nujol): 2189.0 (m), 2129.2 (vs), 2094.5 (s) cm^{-1}. The Optic spectrum (10^{-4} M, THF) 2.79 (s), 2.49 (sh) eV. The molar conductivity (10^{-3} M, acetone) 30.7 Ω^{-1} cm^2 mol^{-1}.

Preparation of [Fe(mnt)(bipy)(*t*-BuNC)$_2$] (2)

Reaction of $FeBr_2$ (0.263 g; 1.22 mmol) with Na_2mnt (0.227 g, 1.22 mmol) and bipy (0.190 g; 1.22 mmol) and *t*-BuNC (0.27 cm^3; 2.44 mmol) as above gave **2** as a brown solid. Yield 47%. (Found: C, 53.9; H, 4.2; N, 15.9. $C_{22}H_{26}S_2FeN_6$ requires C, 55.6; H, 5.0; N, 16.2%). IR ν(CN) (Nujol): 2189.0 (m), 2142.7 (vs), 2110.0 (vs) cm^{-1}. The optic spectrum (2.2 10^{-4} M, THF) 2.95 (s) eV. The molar conductivity (10^{-3} M, acetone) 16.0 Ω^{-1} cm^2 mol^{-1}.

*e-mail: morigaki@npd.ufes.br

Methods and calculations details

The DFT calculations have been performed with the versions ADF2006/2007 program packages of the Amsterdam Density Functional,[11,12] using the combination of exchange functional of Becke[13] and the correlation functional of Perdew[14] (BP86). Scalar relativistic effects have been considered using the zero-order regular approximation (ZORA).[15,16] The $(1s2s2p)^{10}$ frozen core electrons for Fe and S atoms (ADF database TZP), and the $(1s)^2$ for C, and N atoms (ADF database DZP) were used in all calculations. In all cases, the subsequent steps after the geometry optimization in gas phase, were performed the electric field gradient (EFG) on the Fe atom and the analytical vibration frequency calculations. The investigations of UV-visible spectroscopic properties have been carried out with the TD-DFT (30 lowest spin-singlet-allowed transitions were taken into account) in gas phase. The metal-ligand energy interactions[17,18] of **1** and **2** with two isocyanides *t*-BuNC ligands have been proceeded with the ADF suite at the same BP86 level, using geometry optimized in gas phase.

The geometry optimizations and frequency calculations of **1** and **2** with a degree of similitude result with other program were also calculated by the Gaussian 2003W program (G03),[19] employing the spin-restricted formalism of the hybrid functional B3LYP (Becke's three-parameter functional[20] with the LYP[21] correlation functional), in conjunction with LANL2DZ[22] basis set for all atoms. The optimized molecular geometries have confirmed the true energy minima by observation of only positive eigenvalues in the Hessian matrixes. The EFG and $\rho_0(0)$ (electron density at the nucleus)[23] of **1** and **2** were carried out with the program package ORCA,[24] using for the Fe atom a TZV(P)[25] and for the other atoms a DZV(P) basis set.[26]

RESULTS AND DISCUSSION

The elemental analysis data of the microcrystalline isolated products synthesized correspond to the formulation of **1** and **2**, according to Scheme 1.

$$FeBr_2 + Na_2mnt + L + 2\ t\text{-}BuNC \xrightarrow{THF} [Fe(mnt)(L)(t\text{-}BuNC)_2] + 2\ NaBr$$

Scheme 1. *Reaction in THF at room temperature (L = phen or bipy)*

Molar conductivity values have defined their neutral nature, because are in the typical region of a non-electrolyte compound (30.7 and 16.0 Ω^{-1} cm^2 mol^{-1} in acetone for **1** and **2**).[27] Since they are poor soluble and slowly decomposed in polar solvents, precluded measurements of the solvatochromic of absorption bands.

Mössbauer parameters (Table 1) of compounds have been a good indicator of oxidation state, covalence, and geometrical features.[23,28,29] In particular, ^{57}Fe-Mössbauer spectra of various octahedral complexes with the alternative *trans* configuration show a quadrupole splitting (ΔE_Q) twice as big as the ones given by complexes in the *cis* configuration.[30,31] Therefore, ΔE_Q are assigned the *cis* position of two isocyanides in an octahedral environment. Both *cis*-isomers and that the two forms of *cis* and *trans* isomers could not coexist in the material described above.[32,33]

The isomer shifts (δ) (Figure 1) have compatible values of a diamagnetic Fe(II) atom, mainly when they are plotted in a described standard curve,[23] or compare simply to the higher value for the $FeBr_2$ precursor (1.34 mm s^{-1}).[34]

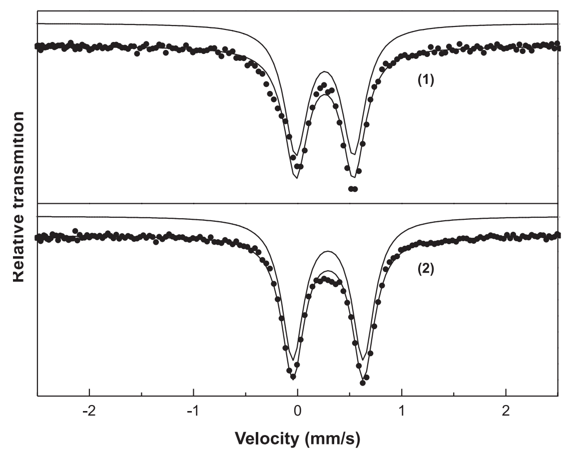

Figure 1. *Mössbauer spectrum of [Fe(mnt)(phen)(t-BuNC)$_2$] (1) and [Fe(mnt)(bipy)(t-BuNC)$_2$] (2) at 80 K*

Acceptable IR data have been extensively used for understanding of many inherent molecular properties,[35] mainly for structure prediction.[36-39] Since IR bands were calculated of the *cis*-isomer can distinguish from the alternative *trans* configuration (Table 1). The experimental of **1** and theoretical IR spectra in the CN stretching frequency region of *trans* and *cis* isomers were compared in Figure 2. Two intense CN stretching bands of near intensity at 2129 and 2095 cm^{-1} indicate that isocyanide ligands reside at the *cis* disposition on the Fe(*t*-BuNC)$_2$ molecular fragment in the IR experimental spectra. The another ν(CN) bands at 2189 cm^{-1} is

Table 1. Theoretical calculations of Mössbauer parameter[a], ν(CN) vibration[b] and energy[c]

Compound	Mössbauer Parameter		ν(CN)(cm^{-1})		Energy	
	δ (mm/s)	ΔE_Q (mm/s)	mnt	*t*-BuNC	Δ_T (kcal/mol)[c]	GAP (eV)
cis-[Fe(mnt)(phen)(*t*-BuNC)$_2$]	0.27(0.26)[d]	0.57(0.56)[d]	2225	2200, 2175	-9717	0.48
trans-[Fe(mnt)(phen)(*t*-BuNC)$_2$]	0.34	0.92	2226	2191	-9710	0.56
cis-[Fe(mnt)(bipy)(*t*-BuNC)$_2$]	0.26(0.30)[d]	0.63(0.68)[d]	2230	2190, 2160	-9258	0.53
trans-[Fe(mnt)(bipy)(*t*-BuNC)$_2$]	0.33	0.93	2226	2191	-9252	0.62

[a]ORCA calculation, [b]B3LYP/LANL2DZ in G03 calculation, [c]Δ_T = total bonding energy in ADF calculation, [d] relative experimental data to room temperature natural-abundance α-Fe at 80 K.

near of the values observed of mnt free, and isocyanide (2134 cm^{-1}) precursors.[40] Similar trend is observed for **2** with the bipy ligand shifts the two ν(CN) isocyanide bands to higher wavenumber at 2143 and 2110 cm^{-1}. Since bipy is the better electron-deficient nature than the phen ligand, there is a decreased in the degree of the back *π-bonding of Fe to isocyanides. More complete IR spectra of compounds **1** and **2** (Figures 1S and 2S, respectively) are available in supplementary material.

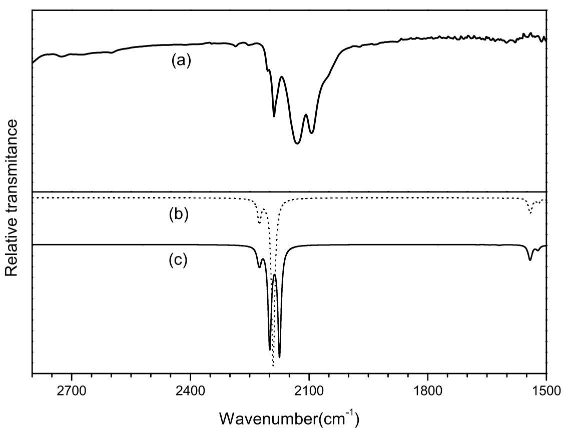

Figure 2. *Infrared Spectrum of [Fe(mnt)(phen)(t-BuNC)$_2$] (1) obtained experimentally (a) and calculated for the trans-1 (b) and cis-1 (c) isomers in the CN stretching region*

The thermogravimetric fragmentation of **1** and **2** occurs with a simultaneous loss of the two isocyanides at the same temperature (109.5 and 138.9 °C, respectively), according to the Scheme 2 and ***(Table*** 2). Since the calculation of the metal-ligand interaction energy is useful for describing the nature of the chemical bonding,[41,42] there is reasonable agreement between TG measures with *t*-BuNC moieties *trans* to Fe-N and Fe-S bonds in the *cis*-**1** and *cis*-**2** structural models, dissociating from the coordination sphere around the same energy (-68 kcal mol^{-1}).

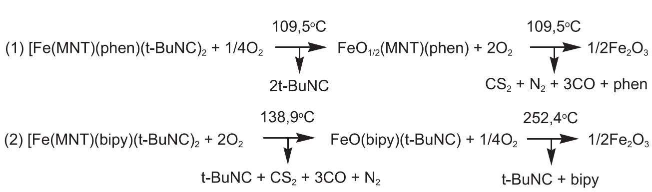

Scheme 2. *Thermal decomposition of [Fe(mnt)(phen)(t-BuNC)$_2$] (1) and [Fe(mnt)(bipy)(t-BuNC)$_2$] (2)*

Although slight the difference thermodynamic stabilization energy between optimized geometries (Figure 3 and Figure 3S), the data suggests that the pseudo octahedral Fe(II) arrangement has two mutually neighbors isocyanides for **1** and **2** in the *cis*-isomer (7 kcal mol^{-1} for L = phen and 6 kcal mol^{-1} for L = bipy). The *cis* conformation of isocyanides maximizes the π* back-bonding, because are pointed mainly at d_x, *d*y, and d_z orbitals direction, while the *trans-isomer* the orbitals are mainly in $d_z{}^2$ and $d_{x^2-y^2}$ direction. The bond lengths average of Fe-C, Fe-N and Fe-S values fit well with those experimentally obtained in the literature[43-50] for $[Fe(S_2C_6H_4)_2]^{2-}$ (2.205 Å of Fe-S),[51] $[\{Fe(mnt)_2\}_2]^{2-}$ (2.230 Å of Fe-S).[52] Furthermore, the reaction has proceeded in a short time,[53] and the intrinsic reaction coordinate calculation of **1** show some rupture of the ligand in the compounds, what suggesting that the *cis-trans* isomerism process is difficult to happen.

The UV-visible absorption spectra of **1** (Figure 4) and **2** (Figure 4S) in THF are dominated by intense transitions in the visible region, and undergo a small red shift when bipy (2.95 eV) is replaced by phen (2.79 eV). The results of calculations and experimental data are good. The TD-DFT formalism was used for determining the electronic

Table 2. TG data for the thermal decompositions of compounds 1 and 2 under oxygen flow

Step	Temperature (°C) Initial - final	Lost Mass (calcd.) (mg)	Lost residue
[Fe(mnt)(phen)(*t*-BuNC)$_2$] (1)			
1	109.5 – 244.0	2.87 (2.93)	2*t*-BuNC-1/4O_2[a]
2	295.0 – 502.1	5.67 (5.65)	Phen + CS_2 + N_2 + 3CO - 1/2O_2[a]
3	900	1.50 (1.48)[b]	1/2Fe_2O_3[b]
[Fe(mnt)(bipy)(*t*-BuNC)$_2$] (2)			
1	138.9 – 252.4	3,52(3.64)	*t*-BuNC + CS_2 + 3CO + N_2 - ½ O_2
2	252.4 – 548.2	4.16(4.06)	*t*-BuNC + bipy - ¼ O_2
3	900.0	1.41(1.43)[b]	1/2Fe_2O_3[b]

[a]acquired element; [b]residue at 900 °C

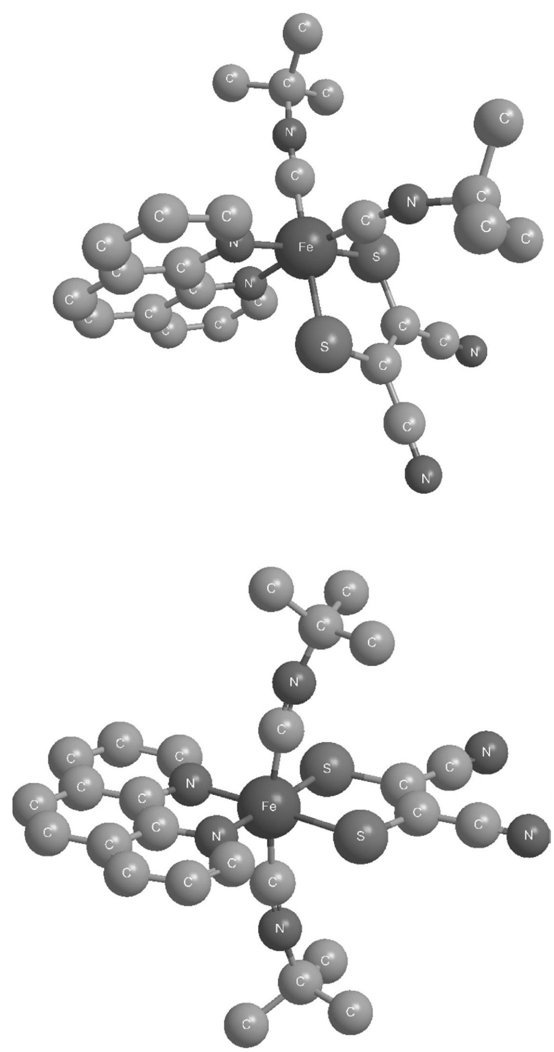

Figure 3. *Optimized Structure of cis and trans [Fe(mnt)(phen)(t-BuNC)$_2$] (hydrogen atom was omitted)*

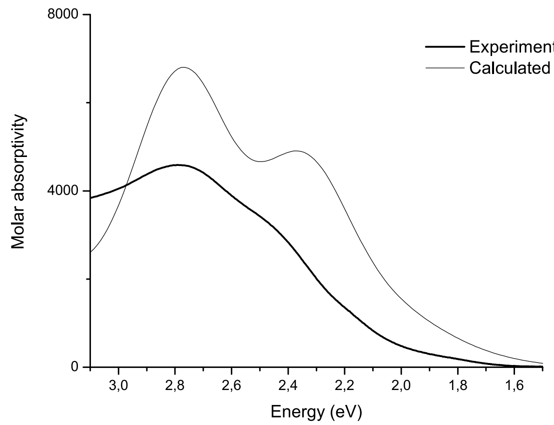

***Figure 4.** Absorption Spectrum of **1** and computed TD-DFT of the cis-**1** isomer*

contributions to MOs, in order to assign the absorption bands and verify preferred isomer formation. The experimental **1** and theoretical *cis*-**1** spectra were combined show two main spectral features with a diffused shoulder of the band I at range 2.53-2.25 eV in the visible region and a more intense band II at 2.79 eV.

Energies, frontier orbitals, and the character of the calculated bands of iron *cis*-**1** and *cis*-**2** isomers are summarized in Table 3 and illustrated in Figure 5. The strongest absorption bands $d \rightarrow \pi^*$ charge transfer are largely located on Fe orbitals from all frontier orbitals with increased in sizable contributions from sulphur atoms *p* orbitals on dithiolate donor with a simultaneous decreased in percentages from the Fe-localized *d* orbitals in two highest-occupied HOMO/HOMO-1 orbitals. May be, the mixture of Fe and dithiolate orbitals force the HOMO orbital nature becomes quasi-nonbonding

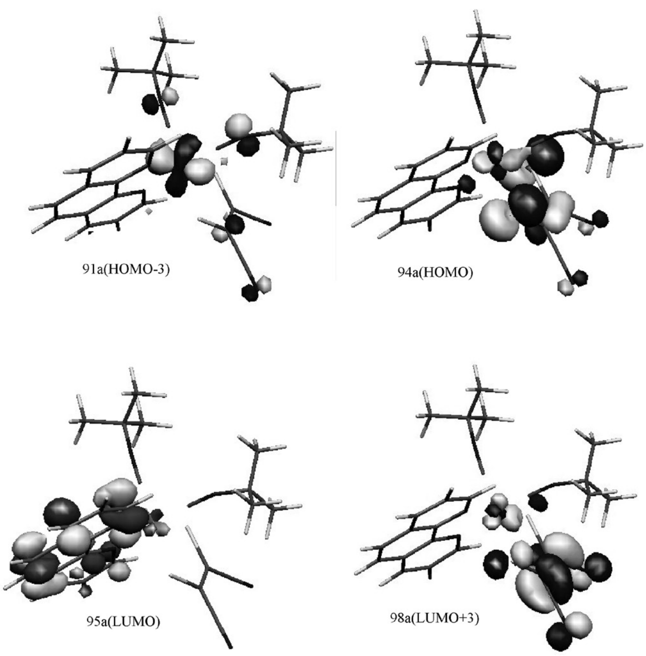

***Figure 5.** Isodensity surface plot (isodensity contour = 0.05) of the 91a (HOMO-3), 94a (HOMO), 95a (LUMO) and 98a (LUMO+3) orbitals to the cis-**1** isomer*

Table 3. Computed the main energies and percentage composition of the highest occupied and lowest unoccupied main atomic orbitals. Contribution from Fe (*d*), mnt (S, *p*), *t*-BuNC (N, *p*), phen and bipy (C, *p*) fragments. Contribution Excitation Energies E_{exc} with Oscillator Strengths ($f \geq 0.01$) for the Optical Transitions of the *cis*-[Fe(mnt)(phen)(*t*-BuNC)$_2$] and *cis*-[Fe(mnt)(bipy)(*t*-BuNC)$_2$] complexes

MO	E (eV)	Fe	mnt	*t*-BuNC	L[a]	MO virtual	E_{exc} (eV)
***cis*-[Fe(mnt)(phen)(*t*-BuNC)$_2$ (*cis*-1)**							
HOMO-5 (89a)	-6.52	10	56	5	0	95a, 96a	2.72, 2.89
HOMO-4 (90a)	-6.42	9	43	7	2	96a	2.74
HOMO-3 (91a)	-5.87	58	3	11	2	95a, 96a, 97a	2.16, 2.34, 3.38
HOMO-2 (92a)	-5.62	69	1	7	6	98a	3.51
HOMO-1 (93a)	-5.33	49	25	3	0	99a	3.45
HOMO (94a)	-4.32	12	60	0	0	98a, 99a, 104a	2.76, 2.32, 3.56
LUMO (95a)	-3.81	3	0	0	67		
LUMO+1 (96a)	-3.75	1	0	0	70		
LUMO+2 (97a)	-3.56	1	0	0	75		
LUMO+3 (98a)	-2.14	3	15	0	0		
LUMO+4 (99a)	-2.10	46	17	0	0		
***cis*-[Fe(mnt)(bipy)(*t*-BuNC)$_2$] (*cis*-2)**							
HOMO-4 (86a)	-6.45	22	47	5	0	91a, 92a	2.67, 3.38
HOMO-3 (87a)	-5.93	58	3	11	0	91a, 93a	2.26, 3.19
HOMO-2 (88a)	-5.69	69	2	6	5	92a, 93a, 94a	2.72, 3.05, 3.54
HOMO-1 (89a)	-5.39	51	24	3	0	95a	3.54
HOMO (90a)	-4.35	13	59	0	0	94a, 95a	2.26, 2.72
LUMO (91a)	-3.82	4	2	0	67		
LUMO+1 (92a)	-3.11	1	0	0	76		
LUMO+2 (93a)	-2.82	0	0	0	73		
LUMO+3 (94a)	-2.20	29	18	0	0		
LUMO+4 (95a)	-2.14	22	11	0	0		

[a]L= phen or bipy

or antibonding. The back-donation are to three lowest-unoccupied LUMOs that have essentially characters of π* acceptor orbitals on the diimine carbon atoms (L). The allowed back-donation to isocyanides is mainly from HOMO orbital to the highest energies LUMO-3/LUMO-4.

The main difference observed between *cis* and *trans* isomers is that the HOMO $d \rightarrow d$ transitions in the *cis*-isomer is preferentially dominated by Fe orbitals, reaching to high levels LUMOs. However, the *trans*-isomer has L and Fe orbitals in degenerate or quasi-degenerate levels in the LUMO/LUMO+1.

CONCLUSION

In conclusion, we have synthesized and characterized novel complexes of formula [Fe(mnt)(L)(*t*-BuNC)$_2$] (L = phen, bipy) from the reaction of $FeBr_2$ with dithiolate, α-diimine L, and isocyanide reagents in THF at room temperature. The electronic, structural and spectroscopy proprieties of the product have been experimentally investigated for a better characterization, providing a good agreement by means of combined DFT theoretical calculations. The main result has defined an octahedral structure with a *cis* configuration of the two isocyanide ligands around iron centre in [Fe(mnt)(L)(*t*-BuNC)$_2$] complexes. Furthermore, the interplay between from mixed dithiolate-to-ligand and metal-to-ligand transitions instead of the typical MLCT transition should be of great fundamental interest.

SUPPLEMENTARY MATERIAL

The Figures 1S to 4S, showing infrared spectrum of **1** and **2** products in 2800-600 cm^{-1} region, optimized structure for *cis*-**2** and *trans*-**2** isomers and absorption spectrum of *cis*-**2** isomer are available on http://quimicanova.sbq.org.br.

ACKNOWLEDGMENTS

This work was supported by the CNPq and FAPESP.

REFERENCES

1. See references in: Makedonas, C.; Mitsopoulou, C. A.; Laholz, F. J.; Balana, A. I.; *Inorg. Chem.* **2003**, *42*, 8853.
2. Zuleta, J. A.; Bevilacqua, J. M.; Proserpio, D. M.; Harvey, P. D.; Eisenberg, R.*; Inorg. Chem.* **1992**, *31*, 2396; Connick, W. B.; Geiger, D.; Eisenberg, R.; *Inorg. Chem*. **1999**, *38*, 3264.
3. Torres, R. A.; Lovell, T.; Noodleman, L.; Case, D. A.; *J. Am. Chem. Soc*. **2003**, *125*, 1923.
4. Müller-Westerhoff, U. T.; Vance, B.; Yoon, D. I.; *Tetrahedron* **1991,** *47*, 909.
5. Beinert, H.; *J. Biol. Inorg. Chem.* **2000**, *5*, 2.
6. Hamilton, W. C.; Bernal, I.; *Inorg. Chem.* **1967**, *6*, 2003; Kanatzidis, M. G.; Coucouvanis, D.; *Inorg. Chem.* **1984**, *23*, 403.
7. Morigaki, M. K.; da Silva, E. M.; de Melo, C. V. P.; Larica, C.; Biondo, A.; Freitas, J. C. C.; Dias, G. H. M.; Ribeiro, H. R.; *Quim. Nova* **2004,** *27*, 76.
8. Gokel, G. W.; Widera, R. P.; Weber, W. P.; *Org. Synth*. **1976**, *55*, 96.
9. Wold, A.; Ruff, J. K.; *Inorg. Synth*. **1973**, *14*, 102.
10. Davison, A.; Holm, R. H.; *Inorg. Synth.* **1967**, *10*, 8; Locke, J.; McCleverty, J. A.; *Inorg. Chem*. **1966**, *5,* 1156.
11. Bickelhaupt, F. M.; Baerends, E. J.; *Rev. Comput. Chem.* **2000**, *15*, 1.
12. Velde, G.T.; Bickelhaupt, F. M.; Baerends, E. J.; van Gisbergen, S. J. A.; Fonseca Guerra, C.; Snijders, J. G.; Ziegler, T. J.; *Rev. Comput. Chem.* **2001**, 22, 931.
13. Becke, A. D.; *Phys. Rev. A* **1988**, *38*, 3098.
14. Perdew, J. P.; *Phys. Rev. B* **1986**, *33*, 8822.
15. Snijders, J. G.; *Mol. Phys*. **1978**, *36*, 1789.
16. Snijders, J. G.; Ros, P.; *Mol. Phys.* **1979**, *38*, 1909.
17. Morokuma, K.; *J. Chem Phys*. **1971**, *55*, 1236.
18. Ziegler; T.; Rauk, A.; *Theor. Chim. Acta* **1977**, *46*, 1.
19. Frisch, M. J.; Trucks, G. W.; Schlegel, H. B.; Scuseria, G. E.; Robb, M. A.; Cheeseman, J. R.; Montgomery Jr., J. A.; Vreven, T.; Kudin, K. N.; Burant, J. C.; Millam, J. M.; Iyengar, S. S.; Tomasi, J.; Barone, V.; Mennucci, B.; Cossi, M.; Scalmani, G.; Rega, N.; Petersson, G. A.; Nakatsuji, H.; Hada, M.; Ehara, M.; Toyota, K.; Fukuda, R.; Hasegawa, J.; Ishida, M.; Nakajima, T.; Honda, Y.; Kitao, O.; Nakai, H.; Klene, M.; Li, X.; Knox, J. E.; Hratchian, H. P.; Cross, J. B.; Adamo, C.; Jaramillo, J.; Gomperts, R.; Stratmann, R. E.; Yazyev, O.; Austin, A. J.; Cammi, R.; Pomelli, C.; Ochterski, J. W.; Ayala, P. Y.; Morokuma, K.; Voth, G. A.; Salvador, P.; Dannenberg, J. J.; Zakrzewski, V. G.; Dapprich, S.; Daniels, A. D.; Strain, M. C.; Farkas, O.; Malick, D. K.; Rabuck, A. D.; Raghavachari, K.; Foresman, J. B.; Ortiz, J. V.; Cui, Q.; Baboul, A. G.; Clifford, S.; Cioslowski, J.; Stefanov, B. B.; Liu, G.; Liashenko, A.; Piskorz, P.; Komaromi, I.; Martin, R. L.; Fox, D. J.; Keith, T.; Al-Laham, M. A.; Peng, C. Y.; Nanayakkara, A.; Challacombe, M.; Gill, P. M. W.; Johnson, B.; Chen, W.; Wong, M. W.; Gonzalez, C.; Pople, J. A.; *Gaussian;* Gaussian, Inc., Pittsburgh PA, 2003.
20. Becke, A. D.; *J. Chem. Phys*. **1993**, *98*, 5648.
21. Lee, C.; Yang, W.; Parr, R. G.; *Phys. Rev. B* **1988**, *37*, 785.
22. Hay, P. J.; Wadt, W. R.; *J. Chem. Phys.* **1985***, 82*, 299.
23. Neese, F.; *Inorg. Chim. Acta* **2000**, *337*, 181.
24. Neese, F.; *ORCA – an ab initio, Density Functional and Semi-empirical Program Package*, Version 2.2, Revision 73.
25. Schäfter, A.; Horn, H.; Ahlrichs, R.; *J. Chem. Phys.* **1992**, *97*, 2571.
26. Godbout, N.; Salahub, D. R.; Andzelm, J.; Wimmer, E.; *Can. J. Chem.* **1992**, *70*, 560.
27. Geary, W. J.; *Coord. Chem. Rev.* **1971**, *7*, 81.
28. Gütlich, P.; Link, R.; Trautwe, A. *In Mössbauer Spectroscopy and Transition Metal Chemistry;* Springer: Heildelberg, 1978.
29. Bläs, R.; Guillin, J.; Bominaar, E. L.; Grodzicki, M.; Marathe, V. R.; Trautwein, A. X.; *J. Phys. B: At. Mol. Phys.* **1987**, *20*, 258; Paulsen, H.; Kröckel, M.; Grodzicki, M.; Bill, E.; Trautwein, A. X.; Leight, G. J.; Solver, J.; *Inorg. Chem.* **1995**, *34*, 6244; Lougear, A.; Grodzicki, M.; Bertoldi, C.; Trautwein, A. X.; Steiner, K.; Amthauer, G.; *Phys. Chem. Miner.* **1999**, *27*, 258; Grodzicki, M.; Flint, H.; Winkler, H.; Walker, A.; Trautwein, A. X.; *J. Phys. Chem.* **1997**, *A101*, 4202.
30. Berrett, R. R; Fitzsimmons, B. W.; *J. Chem. Soc.(A)* **1967**, 525.
31. Brancroft, G. M.; Libbey, E. T.; *J. Chem. Soc., Dalton Trans.* **1973**, 2103.
32. Calogero, S.; Russo, U.; Conderelli, L. L.; Fraga, I.; *Transition Met. Chem.* **1979**, *4*, 156.
33. Souza, G. P.; Konzen, C.; Ardissom, J. D.; De Abreu, H. A.; Duarte, H. A.; Alcântara, A. F. C.; Nunes, W. C.; Macedo, W. A. A.; Knobel, M.; Stumpf, H. O.; *J. Braz. Chem. Soc.* **2006**, *17*, 1534.
34. Greenwood, N. N.; Gibb, T. C.; *Mössbauer Spectroscopy*, 1st ed., Chapman and Hall: London, 1971, p. 117.
35. Koch, W.; Holthausen, M. C.; *A Chemist's guide to Density Functional Theory*, Wiley-VCH, Weinheim, 2000.
36. Wolff, S. K.; *Int. J. Quantum Chem*. **2005**, *104*, 645.
37. Bérces, A; Ziegler, T.; *Top Curr. Chem.* **1996**, *182*, 14.
38. Fournier, R.; Papai, I. In *Recent Advances in Density Functional Methods, part I*, Chong, D. P., ed.;World Scientific: New York, 1996.
39. Sosa, C.; Andzelm, J.; Elkin, B. C.; Wimmer, E.; Dobbs, K. D.; Dixon, D. A.; *J. Phys. Chem.* **1992**, *96*, 6630.
40. Billig, E.; Williams, R.; Bernal, I.; Waters, J. H.; Gray, H. B.; *Inorg. Chem.* **1964**, *5*, 663.

41. Dietz, O.; Rayón, V. M.; Frenking, G.; *Inorg. Chem.* **2003**, *42*, 4977; Loschen, C.; Frenking, G.; *Inorg. Chem.* **2004**, *43*, 778.
42. Massera, C.; Frenking, G.; *Organometallics* **2003**, *22*, 2758.
43. Miller, J.; Balch, A. L.; Enemark, J. H.; *J. Am. Chem. Soc.* **1971**, *93,* 4613.
44. Hulme, R.; Powell, H. M.; *J. Chem. Soc.* **1957**, 719.
45. Joshi, K. K.; Mills, O. S.; Pauson, P. L.; Shaw, B. W.; Stubbs, W. H.; *Chemical Communications* **1965**, 181.
46. Wilford, J. B.; Smith, N. O.; Powell, H. M.; *J. Chem. Soc.(A)* **1968**, 1544.
47. Duboc-Toia, C.; Menage, S.; Vincent, J. M.; Averbuch-Pouchot, M. T.; Fontecave, M.; *Inorg. Chem.* **1997**, *36*, 6148.
48. Gama, V.; Henriques, R. T.; Bonfait, G.; Pereira, C. L.; Waerenborgh, J. C.; Santos, I. C.; Duarte, M. T.; Cabral, J. M. P.; Almeida, M.; *Inorg. Chem.* **1992**, *31*, 2598.
49. Epstein, E. F.; Bernal, I.; *Inorg. Chim. Acta* **1977**, *25*, 145.
50. Miyamae, H.; Sato, S.; Saito, Y.; Sakai, K.; Fukuyama, M.; *Acta Crystallogr*. **1977**, *B33*, 3942.
51. Sellmann, D.; Kleffmann, U. K.; Zapf, L.; Huttner, G.; Zsolnai, L.; *J. Organomet. Chem.* **1984**, *263*, 321.
52. Hamilton, W. C.; Bernal, I.; *Inorg. Chem.* **1967**, *6*, 2003.
53. Nazeeruddin, K.; Zakeerundin, S. M.; Humphry-Baker, R.; Gorelsky, S. I.; Lever, A. B. P.; Grätzel, M.; *Coord. Chem. Rev.* **2000**, *208*, 213.